Quaternary Science Reviews 172 (2017) 44–54

Contents lists available at ScienceDirect

Quaternary Science Reviews

journal homepage: www.elsevier.com/locate/quascirev

Hydrological and ecological changes in western Europe between 3200 and 2000 years BP derived from lipid biomarker δD values in lake Meerfelder Maar sediments

O. Rach [a, b, *], S. Engels [c], A. Kahmen [d], A. Brauer [e], C. Martín-Puertas [e, f], B. van Geel [g], D. Sachse [a]

[a] GFZ German Research Centre for Geosciences, Section 5.1, Geomorphology, Organic Surface Geochemistry Lab, Telegrafenberg, D-14473 Potsdam, Germany
[b] Institute for Earth- and Environmental Science, University of Potsdam, Karl-Liebknecht-Strasse 24-25, 14476 Potsdam, Germany
[c] Centre for Environmental Geochemistry, School of Geography, University of Nottingham, University Park, Nottingham, UK
[d] Botany – Department of Environmental Sciences, University of Basel, Schönbeinstrasse 6, 4056 Basel, Switzerland
[e] GFZ German Research Centre for Geosciences, Section 5.2 Climate Dynamics and Landscape Evolution, Telegrafenberg, 14473 Potsdam, Germany
[f] Department of Geography, Royal Holloway, University of London, Egham, Surrey TW20 0EX, UK
[g] Institute for Biodiversity and Ecosystem Dynamics, University of Amsterdam, Science Park 904, 1098 XH Amsterdam, The Netherlands

ARTICLE INFO

Article history:
Received 16 March 2017
Received in revised form
21 June 2017
Accepted 22 July 2017

Keywords:
Holocene
Climate dynamics
Paleoclimatology
Western Europe
Continental biomarkers
Organic geochemistry
Stable isotopes
Vegetation dynamics

ABSTRACT

One of the most significant Late Holocene climate shifts occurred around 2800 years ago, when cooler and wetter climate conditions established in western Europe. This shift coincided with an abrupt change in regional atmospheric circulation between 2760 and 2560 cal years BP, which has been linked to a grand solar minimum with the same duration (the Homeric Minimum). We investigated the temporal sequence of hydroclimatic and vegetation changes across this interval of climatic change (Homeric climate oscillation) by using lipid biomarker stable hydrogen isotope ratios (δD values) and pollen assemblages from the annually-laminated sediment record from lake Meerfelder Maar (Germany).

Over the investigated interval (3200–2000 varve years BP), terrestrial lipid biomarker δD showed a gradual trend to more negative values, consistent with the western Europe long-term climate trend of the Late Holocene. At ca. 2640 varve years BP we identified a strong increase in aquatic plants and algal remains, indicating a rapid change in the aquatic ecosystem superimposed on this long-term trend. Interestingly, this aquatic ecosystem change was accompanied by large changes in δD values of aquatic lipid biomarkers, such as nC_{21} and nC_{23} (by between 22 and 30‰). As these variations cannot solely be explained by hydroclimate changes, we suggest that these changes in the δD_{aq} value were influenced by changes in *n*-alkane source organisms. Our results illustrate that if ubiquitous aquatic lipid biomarkers are derived from a limited pool of organisms, changes in lake ecology can be a driving factor for variations on sedimentary lipid δD_{aq} values, which then could be easily misinterpreted in terms of hydroclimatic changes.

1. Introduction

Late Holocene climate was characterized by a gradual long-term cooling trend recognized globally (Marcott et al., 2013; Wanner et al., 2008), but also by superimposed short-term climatic variations occurring over the lifetime of a few generations and with strong impact on regional climate and society. For example, a relatively abrupt cooling and increased humidity 2800 years ago in the North Atlantic-European region (Swierczynski et al., 2013; Wirth et al., 2013) were interpreted from peat bog records in the Netherlands (van Geel et al., 1996; van Geel et al., 1999), glacial advances, and increased lake levels throughout Europe (e.g. Magny,

* Corresponding author. GFZ German Research Centre for Geosciences, Section 5.1, Geomorphology, Organic Surface Geochemistry Lab, Telegrafenberg, D-14473 Potsdam, Germany.
E-mail address: oliver.rach@gfz-potsdam.de (O. Rach).

http://dx.doi.org/10.1016/j.quascirev.2017.07.019
0277-3791/

1993; Engels et al., 2016a). This change (Movius, 2013) coincided with a significant shift in the western Europe landscape that marked the onset of the Subatlantic period (Litt et al., 2001). The climate change 2800 years ago has been related to the occurrence of a grand solar minimum (Magny, 1993; Martin-Puertas et al., 2012b; van Geel et al., 1996; van Geel et al., 1999), the Homeric Minimum, which occurred between 2750 and 2550 cal years BP recognized in both ^{14}C-tree rings (Reimer et al., 2009) and ^{10}Be-Greenland ice core records (Reimer et al., 2009; Vonmoos et al., 2006). Martin-Puertas et al. (2012b) recently reconstructed changes in solar variability during the time interval from 3300 to 2000 years BP by analyzing changes in ^{10}Be accumulation rates in the annually laminated (varved) sediment record of lake Meerfelder Maar (MFM). The authors compared the reconstructed changes in solar variability to changes in windiness (reconstructed from varve thickness) using the sediment record. The study showed a sharp increase (over less than a decade) in both the climatic and solar proxies at 2759 ± 39 varve years BP and a reduction 199 ± 9 years later, indicating that atmospheric circulation reacted abruptly and in phase with the grand solar minimum and hence showing empirical evidence for a solar-induced "Homeric Climate Oscillation" (HCO).

The HCO has been suggested to be the trigger for human migrations during the transition from Bronze Age to Iron Age (Scott et al., 2006; van Geel et al., 1996). Archeological and paleoecological studies from different locations in Europe (e.g. the Netherlands and Germany) also provide evidence for an increase in human activity and reorganization of prehistoric cultures around that time (Kubitz, 2000; van Geel et al., 1996), most likely favored by a rise in human population density after the climate deterioration (van Geel and Berglund, 2000). Although wetter conditions have been inferred for the HCO, it yet remains elusive if these wetter conditions were associated to major changes in rainfall intensity and/or lower evapotranspiration and the possible relation to the observed vegetation changes in western Europe. Furthermore, the exact temporal succession of regional hydrological and environmental changes during this period is unknown due to the lack of highly-resolved hydrological records in western Europe.

In this study we analyze high-resolution lipid biomarker hydrogen isotope ratios of a Late Holocene sedimentary sequence from lake MFM in western Germany to test its potential for elucidating the nature of hydrological changes during the HCO. Stable hydrogen isotope ratios (expressed δD values) of sedimentary lipid biomarkers (i.e. *n*-alkanes), which can be traced back to their biological sources (Eglinton and Eglinton, 2008; Killops and Killops, 2005; Peters et al., 2007; Sachs et al., 2013), have become an important paleohydrological proxy over the last ca. 15 years. This has resulted in new insights into hydroclimate dynamics over different geological timescales (Aichner et al., 2010; Atwood and Sachs, 2014; Feakins et al., 2014; Rach et al., 2014; Sachs et al., 2009; Schefuss et al., 2011; Smittenberg et al., 2011; Tierney et al., 2008, 2010; Zhang et al., 2014). Rach et al. (2014) demonstrated that *n*-alkane δD analyzes are a suitable proxy for reconstructing regional hydrological changes during major and abrupt climate shifts during the Late-Glacial that are recorded in the varved sediments of lake MFM.

Our specific objectives for this study are (1) to reconstruct hydroclimate variations for central-western Europe during a period of changing environmental conditions (3200–2000 varve years BP) using lipid biomarker stable isotope data, and (2) to combine this record with a high-resolution aquatic and terrestrial vegetation reconstruction in order to evaluate possible effects of vegetation change on the biomarker stable isotope record.

2. Lipid biomarkers as paleoclimate proxies

2.1. Sedimentary n-alkanes as biomarkers for aquatic and terrestrial organisms

Straight-chained hydrocarbons such as *n*-alkanes are increasingly applied for paleoclimate reconstruction. Different *n*-alkane homologues are produced by bacteria, aquatic as well as terrestrial plants (Aichner et al., 2010; Baas et al., 2000; Cranwell et al., 1987; Eglinton and Hamilton, 1967; Ficken et al., 2000; Gelpi et al., 1970). As such, *n*-alkanes can be used to obtain information on their biological sources. While not species-specific, different groups of source organisms can be distinguished based on *n*-alkane chain length: *n*-alkanes with 17–19 (nC$_{17}$ - nC$_{19}$) carbon atoms (short-chain) are predominantly synthesized by aquatic algae but also by bacteria (Cranwell et al., 1987; Gelpi et al., 1970; Sachse and Sachs, 2008). Mid-chain *n*-alkanes (nC$_{21}$ - nC$_{25}$) are mainly synthesized by submerged aquatic plants (Aichner et al., 2010; Baas et al., 2000; Ficken et al., 2000). Long-chain *n*-alkanes (nC$_{27}$ - nC$_{31}$) are major components of the leaf waxes of terrestrial higher plants (Eglinton and Hamilton, 1967; Massimo, 1996), although conifers produce significantly smaller amounts of *n*-alkanes than broad-leaved species (Diefendorf et al., 2011). Some terrestrial plants also produce significant amounts of nC$_{25}$, making source assessment for this compound more difficult, but in general aquatic or terrestrial sources can be distinguished from *n*-alkane abundances in sediments (Gao et al., 2011).

2.2. Climatic and environmental influences on δD values of aquatic and terrestrial biomarkers

The observation that δD values of aquatic (δD_{aq}) and terrestrial (δD_{terr}) plant derived lipid biomarkers record the δD values of the organisms' source water (Garcin et al., 2012; Huang et al., 2004; Sachse et al., 2004, 2012; Sauer et al., 2001) has fueled the application of δD measurements as a paleohydrological proxy. The major determinant of the δD values of aquatic and terrestrial lipid biomarkers is the δD value of the source water used by the organism (Sachse et al., 2012). Photosynthetic lacustrine aquatic organisms, such as submerged aquatic macrophytes and algae use lake water as a hydrogen source to synthesize *n*-alkanes. In a closed lake system (in temperate climates), which is only fed by precipitation and characterized by a low precipitation/evaporation ratio, the hydrogen isotope composition of lake water can be interpreted as an integrated signal of precipitation δD (Aichner et al., 2010; Sachse et al., 2012). In particular, for MFM, being a maar with steep catchment walls (sheltered from the wind) an effect of evaporation on lake water is unlikely. For a neighboring maar lake (Holzmaar) a long-term study of lake water has shown that δ^{18}O values vary only around 1‰ and follow the seasonal temperature evolution (Moschen et al., 2005). Thus, in such a lake system sedimentary δD_{aq} values provide an integrated precipitation δD signal (Sachse et al., 2004).

Higher land plants on the other hand directly take up precipitation water (through soil water) (Sachse et al., 2012). However, transpirative processes in the leaf of the plant modify the isotopic composition of water (i.e. increased enrichment in D under drier conditions) before hydrogen is being fed into biosynthetic reactions (Kahmen et al., 2013a, 2013b; Sachse et al., 2012). As a consequence, sedimentary δD_{terr} values also record changes in ecosystem evapotranspiration (Kahmen et al., 2013b; Sachse et al., 2004).

2.3. Species-specific differences and their influence on aquatic and terrestrial lipid δD values

In addition to the isotopic composition of source water, it has been demonstrated that changes in vegetation type (of terrestrial plants) as well as aquatic lipid source organisms can also significantly affect the isotope composition of terrestrial and aquatic lipids (Sachse et al., 2012).

For example, major differences in the net or apparent fractionation ($\varepsilon_{l/w}$), i.e. the isotopic difference between the source water (δD_w) and lipid (δD_l) (eq. (1)), have been observed among different plant functional types (Gao et al., 2014; Sachse et al., 2012).

$$\varepsilon_{l/w} = \frac{(D/H)_l}{(D/H)_w} \quad (1)$$

Since $\varepsilon_{l/w}$ represents the sum of physical and biochemical fractionation processes, it is currently unclear to what extent individual parameters are responsible for the observed differences. For example, major differences in the biosynthetic fractionation (ε_{bio}) between various species as well as differences in leaf-morphology, transpiration and water use efficiency between grasses and broadleaf-woody plants have been shown to affect $\varepsilon_{l/w}$ (Kahmen et al., 2013b; Liu et al., 2006; McInerney et al., 2011; Sachse et al., 2012).

On the other hand, $\varepsilon_{l/w}$ in aquatic algae and cyanobacteria can also be influenced by water salinity and growth rate, possibly related to biochemical processes as shown for *n*-alkanoic acids (Sachs, 2014), the biosynthetic precursors of *n*-alkanes (Eglinton and Eglinton, 2008; Sachse et al., 2012; Sessions et al., 1999). In addition, significant differences in ε_{bio} have been observed among different algae (Zhang and Sachs, 2007). For example, under similar conditions in batch cultures, two different groups of green algae (Chlorophyceae and Trebouxiophyceae) produced C_{16} *n*-alkanoic acids, which differed in their δD values by 160‰ (Zhang and Sachs, 2007). Less information is available for submerged aquatic plants, but studies on modern aquatic plants and lake surface sediments have suggested the ε_{bio} for aquatic macrophytes (i.e. *Potamogeton*) may be significantly smaller (−82‰) (Aichner et al., 2010) than observed for algae (−157‰) (Sachse et al., 2004).

Therefore, if various algae and other water plants produce the same unspecific biomarker (e.g. short-to mid-chain *n*-alkanes) and the aquatic ecosystem (i.e. species composition) changes, the sedimentary *n*-alkane δD record could be affected. In a similar way, major vegetation changes can affect the δD_{terr} signal (Nelson et al., 2013). Despite these complications, δD values of aquatic and terrestrial lipids from sedimentary archives can be used to reconstruct changes in hydroclimate over time, if constraints on the processes discussed above, i.e. information about the terrestrial and aquatic producers of the studied lipids, are available (Aichner et al., 2010; Atwood and Sachs, 2014; Rach et al., 2014).

Therefore, for a robust paleoclimatic interpretation it is important to understand the interplay between hydrological and vegetation change and their effect on sedimentary lipid biomarker δD records. The here studied time interval was characterized by long and short-term climatic change as well as vegetation changes and this provides a testing ground to study the above discussed processes and their influence on biomarker δD values. Therefore, we compare a high-resolution δD_{aq} and δD_{terr} record from lake MFM in western Germany to lake and catchment ecosystem development, inferred from a new pollen-based vegetation reconstruction, as well as published sedimentary proxy data from MFM, such as varve thickness and Ti influx (Martin-Puertas et al., 2012b).

3. Study site

Lake Meerfelder Maar (*50° 06' 2.87" N; 06° 45' 27.13" E*) is located in western Germany as a part of the West-Eifel Volcanic Field (Fig. 1). The lake is situated in a volcanic crater which was formed by a phreatomagmatic eruption 80,000 years ago (Zöller and Blanchard, 2009).

The modern lake is situated at 336.5 m a.s.l. and the lake surface is around 0.248 km^2, covering the northern part (ca. 1/3) of the maar crater surface (Fig. 1). The maximum water depth is 18 m. The southern part of the crater is filled in by a shallow delta plain, deposited from a stream (Meerbach) passing through the crater rim in the south. The lake is eutrophic and due to its particular morphological situation within a deep maar crater, Lake MFM is wind-sheltered, favoring the preservation of fine seasonal layers within the sediment sequence (Brauer et al., 1999a, 2008).

The climate of the region is influenced by its proximity to the North Sea coast (ca. 250 km) with a mean annual air temperature of 8.2 °C and mean annual precipitation of 950 mm, peaking in winter (Martin-Puertas et al., 2012a).

Seven sediment cores were collected in 2009 from the deepest area of Lake MFM using a UWITEC piston core, with a maximum distance between sites of 20 m. The sediment cores, labeled as MFM09-A to MFM09-G, were split, imaged, described and an overlapping sediment profile was constructed (Martin-Puertas et al., 2012a). For the present study the uppermost core MFM09-A was selected for sampling. We studied a meter long sequence from 230 to 330 cm depth, which covers the interval from 2000 to 3200 varve years BP (Martin-Puertas et al., 2012b). The MFM chronology (MFM2000) has been established by varve counting from ca. 1500 cal years BP back to 14,200 cal years BP along 7.85 m of sediments with a cumulative counting error of less than 5% and is supported by 51 radiocarbon dates (Brauer et al., 2000). This independent but floating chronology was anchored to the calendar year time scale by adopting the age of the regional (Eifel) Ulmener Maar Tephra (UMT) for the MFM record (Brauer et al., 1999b, 2000). The UMT is dated at 11,000 ± 110 cal years BP in the Lake Holzmaar (HZM) varve chronology by multiple count sequences and ^{14}C based-correction (Zolitschka et al., 2000). The proximity of Lake HZM to MFM (10 km) provides the opportunity to compare both records, showing a good agreement between the chronologies (Litt et al., 2009). For the study interval, an age error estimate has been provided by combining varve counting, radiocarbon dating and sediment ^{10}Be accumulation rates (Martin-Puertas et al., 2012b). All ages in the following text are rounded on 5 years to avoid interpretations on a temporal accuracy level, which is not supported by the current age model.

4. Methods

4.1. Biomarker extraction, identification and quantification

A 1.0-m-long core section, which included the time interval of the HCO, was sampled in consecutive 1-cm-thick slices, resulting in a total of 100 samples. Due to differences in sedimentation rate, the temporal resolution of the samples varies between 4 and 45 years per sample.

To remove remaining water, all samples were freeze-dried and subsequently homogenized. A Dionex accelerated solvent extraction system (ASE 350) with a dichloromethane (DCM): methanol mixture (9:1) at 100 °C and 103 bar was used for the extraction of lipid biomarkers from freeze-dried samples in the biomarker laboratory at the University of Potsdam. The total lipid extracts (TLE) were separated into three fractions (aliphatic (F1), aromatic (F2) and alcohol/fatty acid (F3)) by solid phase extraction (SPE). The

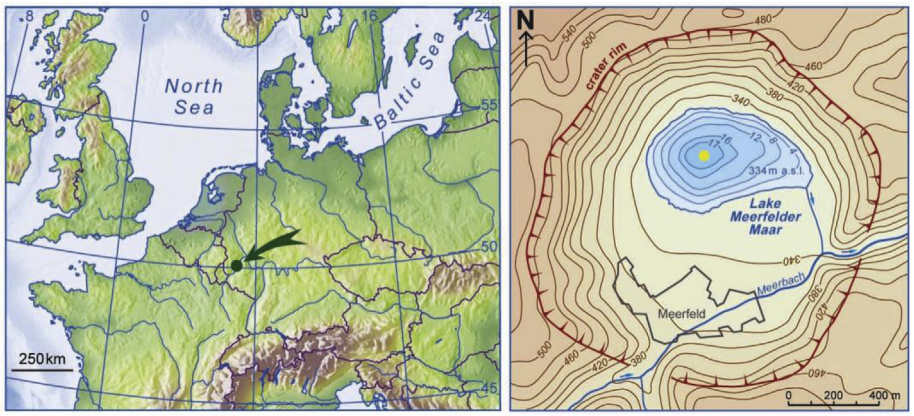

Fig. 1. Map of western Europe with the study locations. Coloured dots mark the study (left) and coring (right) site at MFM. (For interpretation of the references to colour in this figure legend, the reader is referred to the web version of this article.)

separation was achieved using 2 g silica gel as the stationary phase and hexane, hexane:DCM (1:1) and DCM as the respective mobile phases. Activated copper in a pipette column was used to remove elemental sulfur from the F1 fraction. The aliphatic fraction was dominated by *n*-alkanes (nC_{21}-nC_{31} homologues) and alkenes. Fractions F2 and F3 contained mainly ketones, alcohols and fatty acids. To avoid coelution of alkanes and alkenes during isotope measurement, the F1 fraction was further purified using silver nitrate ($AgNO_3$) impregnated silica gel in a pipette column with hexane and dichloromethane as the mobile phase for the elution of alkanes and alkenes, respectively.

n-Alkane identification and quantification was performed using a gas chromatograph (GC 7890-A, Agilent, Santa Clara, USA) coupled to a flame ionization detector (FID) and a mass selective detector (MSD) (MS 5975-C, Agilent, Santa Clara, USA) coupled via an electronic split interface. The quantification was performed through the FID by comparing compound peak area to the peak area of the internal standard (5α-androstane). Compound identification was achieved using the MSD and comparison with library and literature mass spectra. The GC temperature program used for *n*-alkane quantification contained the following specifications: injection at 70 °C (hold for 2 min), then heating up to 140 °C with a ramp of 12 °C per minute directly followed by a heating to 320 °C with a ramp of 2 °C per minute. The final temperature of 320 °C was held for 15 min. The PTV injector started at 50 °C and was heating up to 350 °C with a ramp of 14 °C per second.

4.2. Stable isotope measurement and evaluation

Compound-specific hydrogen isotope ratios of the *n*-alkanes were measured on a Delta-V-Plus Isotope Ratio Mass Spectrometer (IRMS) (Thermo Fisher, Bremer, Germany) coupled to a Trace Gas Chromatograph Ultra (Thermo Fisher, Bremer, Germany) at the Swiss Federal Institute of Technology Zurich (ETH Zurich). The following GC-temperature program was used: start at 90 °C (held for 2 min), heating up to 150 °C with 10 °C per minute, heating from 150 °C to 320 °C with 4 °C per minute; the final temperature was held for 10 min. Each sample was injected three times. For conversion of the measured δD values to the VSMOW scale a standard containing nC_{16} to nC_{30} alkanes (Mix A4 obtained from Arndt Schimmelmann, Indiana University) with known δD values was measured in triplicate at the beginning and the end of each sequence. All measured δD values were corrected to the VSMOW scale using a linear regression function (with a specific slope and intercept) derived from measured vs. real Mix A4 standard values. The mean standard deviation of all A4 standard measurements (n = 441) was 2.1‰, while the mean standard deviation of all sample *n*-alkane measurements (n = 492) was 1.4‰. To avoid misinterpretation of the measured δD values only baseline separated peaks with areas over 20Vs have been used for interpretation. The $H3^+$ factor was determined before each sequence and remained constant at 3.63 ± 0.39 during the 4 weeks measurement period.

4.3. Palynological analysis

Two plastic containers of 35 × 260 mm were pressed into cores MFM09A2DR and MFM09A2UR to a depth of 10 mm. The sediment in the plastic containers was subsequently subsampled with a 3 samples/centimeter resolution for the sediments older than 2765 varve years BP and a 2 samples/centimeter resolution for the sediments younger than 2765 varve years BP. These sampling intervals correspond to a temporal resolution of 1–29 years per sample. Ninety-one samples were prepared for the analysis of pollen and spores at the University of Amsterdam following the protocols of Faegri et al. (1990) and Moore et al. (1991). Standard tablets with *Lycopodium* spores were added to the sample during laboratory processing to estimate pollen and spore concentrations and influx numbers (Stockmarr, 1971). Pollen, fern spores, fungal spores, and other palynomorphs (including remains of freshwater algae) were identified using a light microscope with 400× magnification (1000× when necessary). Keys and illustrations by Moore et al. (1991) and Beug (2004) as well as a reference collection were used for pollen identification. The identification of algal remains and other non-pollen palynomorphs (NPPs) follows Van Geel (1978). A pollen percentage diagram was calculated using a pollen sum (Σ-pollen) that includes arboreal pollen and pollen of upland herbs and the average Σ-pollen is 572 (range: 443–698). The percent-abundances of all pollen, spores and NPPs are calculated in relation to Σ-pollen. Concentrations of individual taxa were calculated by multiplying the number of encountered pollen by the ratio of the number of added *Lycopodium* spores and the number of spores encountered during analysis. This number was then divided by the volume of material used in the analysis to derive taxon-specific pollen concentrations. A percent-abundance diagram was plotted using TILIA v 1.17.6; concentration- and influx-diagrams were plotted using C2. Details on the taxa important for the interpretation of our *n*-alkane data are presented in section 5.3 (pollen data), whereas overview diagrams of the arboreal taxa (percentages, concentrations and influx) (Fig. S1) and the aquatic

taxa (expressed as percentages in relation to Σ-pollen) (Fig. S2) can be found in the Supplementary Information.

5. Results

5.1. n-Alkane concentrations

In total 100 samples were analyzed for their *n*-alkane content. Eighteen samples did not contain enough material for *n*-alkane analysis. In the remaining 82 samples the concentration of all identified *n*-alkanes (nC_{21} to nC_{31}) ranged from 0.34 to 69.42 μg/g dry weight of sediment. The most abundant *n*-alkane homologue in all samples was nC_{29} with an average concentration of 26.5 μg/g sediment dry weight per sample (range 3.0–69.1 μg/g). The compound with the lowest concentration was always nC_{21} with 3.9 μg/g on average (range 0.34–14.3 μg/g). Other *n*-alkanes (nC_{23}, nC_{25}, nC_{27} and nC_{31}) had average concentrations between 4.2 and 20.5 μg/g sediment dry weight. The average chain-length (ACL) varied between 26.0 and 28.8.

The average influx values (μg normalized per varve year) of short- and long-chain *n*-alkanes showed significant variations. Before the HCO, nC_{21} and nC_{23} showed average influx values of 0.35 and 0.27μg/year, while the nC_{25} to nC_{31} homologues showed average influx values between 0.46 and 1.34 μg/year, respectively (Fig. 2B). The influx of nC_{21} and nC_{23} increased rapidly to 0.68 and 1.03μg/year after 2785 varve years BP, while the influx values of nC_{25} to nC_{31} also increased to average values between 2.10 and 6.28 μg/year (Fig. 2B). The average *n*-alkane influx values for nC_{21} and nC_{23} decreased abruptly to average values of 0.12 and 0.15 μg/year after the HCO (Fig. 2B). The nC_{25} to nC_{31} homologues also decreased to average influx values between 0.37 and 1.42μg/year. nC_{21} showed maximum influx values during the first part of the HCO (2750–2660 varve years BP), while long-chain *n*-alkanes had their maximum influx rates in the second part of the HCO (2700–2610 varve years BP) (Fig. 2B). Influx rates of nC_{23} showed local maxima both in the first half of the HCO (at 2740 varve years BP) as well as in the second half of the HCO (at 2610 varve years BP) (Fig. 2B).

5.2. Stable hydrogen isotope composition (δD values) of the n-alkanes

All 82 samples were analyzed for compound specific stable hydrogen isotope ratios, expressed as δD values. The *n*-alkane δD values showed a decreasing trend during the analyzed period (Fig. 2A). Generally, the δD values of all *n*-alkanes were more

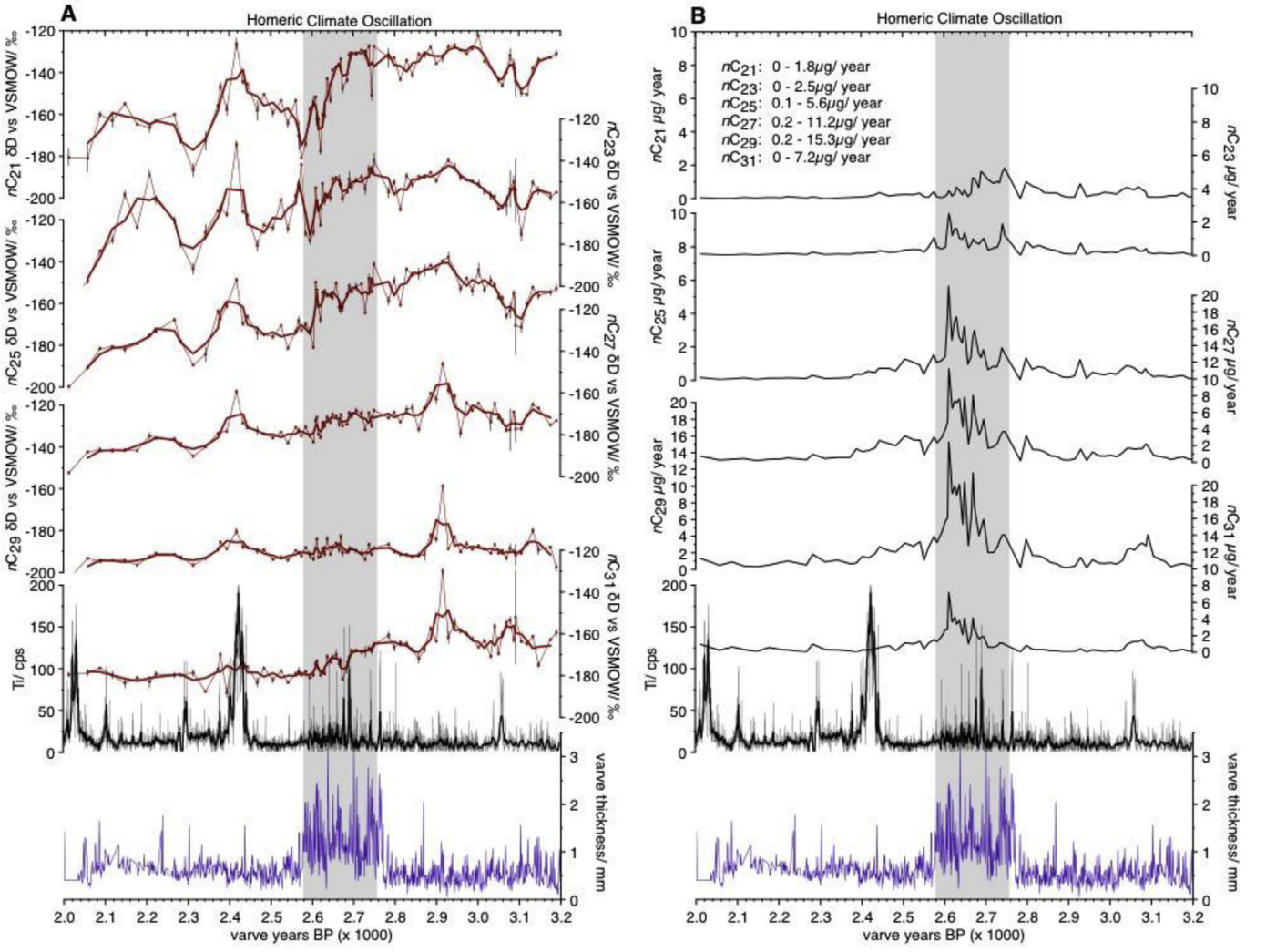

Fig. 2. δD values (A) (smoothing by 3-data running average) and annual flux (μg/year) (B) of nC_{21}-nC_{31} alkanes and varve thickness as well as Titanium content (smoothing by 100-data running average) (Martin-Puertas et al., 2012b) of the studied core section.

positive before the HCO than after (Fig. 2A). However, there were major differences in the magnitude of variation between *n*-alkanes of different chain-length. Short and mid-chain *n*-alkanes (nC_{21}-nC_{25}) generally showed higher variability in their δD values than long-chain *n*-alkanes. Before the HCO, nC_{21} δD values were on average −135 ± 2‰ (arithmetic mean from 3190 to 2785 varve years BP with respective 95% confidence interval) while after the HCO the average δD value changed to −160 ± 5‰ (arithmetic mean from 2540 to 2015 varve years BP). Applying the epsilon equation (Sessions and Hayes, 2005) for accurate calculations of differences in δ-values results in a difference of about 30‰ for nC_{21} δD values before and after the HCO. The average δD values of nC_{23} and nC_{25} for the same period changed from −153 ± 3‰ and −152 ± 3‰ to −171 ± 7‰ and −176 ± 4‰, respectively (difference 22 and 28‰) (Fig. 2A).

Long-chain *n*-alkanes generally showed smaller changes in their δD values. The average δD values of nC_{27} and nC_{29} changed from −169 ± 2‰ and −188 ± 2‰ (before the HCO) to −182 ± 3‰ and −192 ± 2‰ (after the HCO) (difference 15 and 4‰). The δD values of nC_{31} changed from −162 ± 3‰ to −179 ± 2‰ (difference 20‰) (Fig. 2A).

5.3. Pollen-data

The lower part of the pollen record (2945–2795 varve years BP) was characterized by relatively high percentages of arboreal pollen (AP) of 95–100% (Fig. 3). The pollen-assemblages were dominated by *Fagus* which reached abundances >60%, accompanied by relatively high abundances of other deciduous tree taxa such as *Alnus* (15–30%), *Corylus* (5–15%) and *Quercus* (5–15%). Pollen from non-arboreal taxa (NAP) were only present in low abundances between 2945 and 2795 varve years BP, suggesting that the vegetation around MFM consisted of a closed-canopy forest.

A sharp decrease in relative abundance of *Fagus* to values of around 40% was observed at ~2795 varve years BP (Fig. 3). Simultaneously, spores of *Kretzschmaria deusta*, a parasitic fungus living on various tree species (van Geel et al., 2013), showed an increase in abundance to values of 5%. An increase in the relative abundance of *Alnus* as well as of several NAP-taxa coincided with the decrease in *Fagus* (Fig. 3). Crop plants (e.g. Poaceae, Cerealia) as well as *Plantago lanceolata* and *Rumex acetosella-type* all started to increase after 2795 varve years BP. Remains (vegetative cell walls) of the green algae *Botryococcus*, *Tetraedron minimum* and of the aquatic macrophyte *Myriophyllum spicatum*/*verticillatum*-type showed an increase around 2620 and 2595 varve years BP, respectively.

6. Discussion

Our lipid biomarker stable hydrogen isotope record showed a long-term trend to more negative δD values during the 3200 to 2000 varve years BP interval. This is evident in all analyzed biomarkers, regardless of their biological origin (Fig. 2). The decrease in lipid δD values possibly reflects the long-term cooling trend as a consequence of declining summer insolation in the Northern Hemisphere (Marcott et al., 2013; Renssen et al., 2009) in the way that a decrease in air temperature would lead to more negative precipitation δD values (Dansgaard, 1964; Gat, 1996; Gat et al., 2000). However, we observed substantial differences in the magnitude of changes in δD values between aquatic and terrestrial plant derived lipid biomarkers: δD_{aq} values showed a rather abrupt decrease starting at around 2700 varve years BP, a change not observed for δD_{terr} values (except a slight decrease in nC_{31} δD values). This indicates that different processes controlled the observed changes for aquatic and terrestrial biomarkers. While

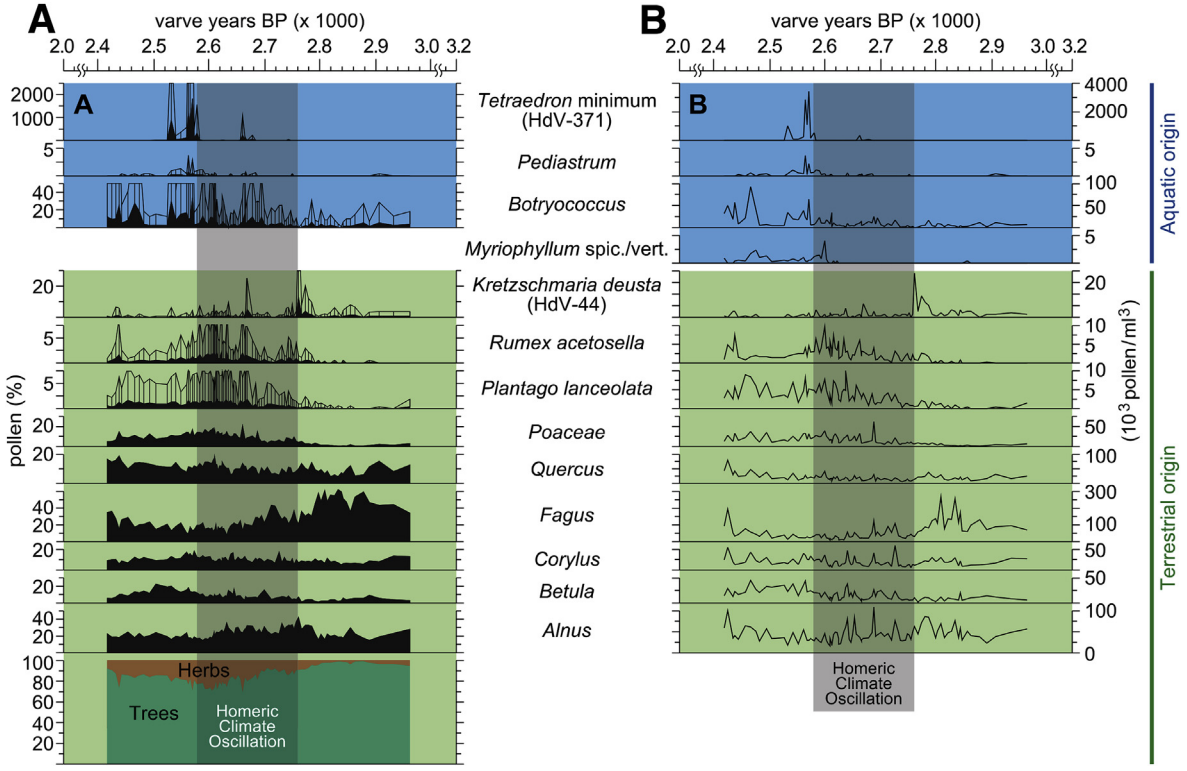

Fig. 3. Pollen and spores abundance of the major constituents of vegetation in and surrounding MFM given in % (A) and pollen concentrations (B). Thinner lines on top of the upper six plots in A marking exaggeration-lines (5-times). Blue shaded areas marking aquatic organisms. Green areas are showing terrestrial plants. The dark-green/orange areas show the local tree/herb distribution in percentage. (For interpretation of the references to colour in this figure legend, the reader is referred to the web version of this article.)

different biosynthetic fractionation factors for aquatic and terrestrial plants can explain different absolute δD values, different magnitudes of change indicate either significant evapotranspirational or ecological changes. For example, cooler and more arid conditions could explain a stronger decrease in δD_{aq} compared to δD_{terr}, as δD_{terr} values would reflect increasing plant transpiration (Kahmen et al., 2013b). However, there is no evidence for a substantial aridification during this period in western Europe. Rather, several studies suggest a shift to more humid conditions during this period (Martin-Puertas et al., 2012b; Van Geel, 1978; van Geel et al., 1996; van Geel et al., 2013). With our combined high-resolution lipid biomarker and palynological analysis we therefore explore ecological changes in the aquatic and terrestrial ecosystem in and around MFM to test if these changes may have influenced the magnitude of change in biomarker δD values.

6.1. Changes in vegetation based on palynological records

The palynological data provide first evidence for changes in the terrestrial ecosystem at ca. 2800 varve years BP. Our pollen record showed a decrease in relative pollen abundance of *Fagus* by half and a doubling of *Alnus,* accompanied by a general trend to increasing grass/herb vegetation in the catchment of MFM (Fig. 3A). The presence/increase of human-impact indicators such as *Plantago lanceolata* and *Rumex acetosella*-type provided evidence for increased human impact (Behre, 1981) in the catchment of MFM. *Kretzschmaria deusta* spores increased in abundance from 2795 to 2765 varve years BP, which could be a result of the temporary occurrence of this fungus on wounded trees that were present in the landscape after the clearing of parts of the forest (Kubitz, 2000; van Geel et al., 2013).

The second substantial decline in tree pollen at 2695 varve years BP occurred about 100 years after the variations mentioned above (Fig. 3A). This marks a second phase of ecosystem changes, which is additionally characterized by an increase of *Botryococcus* – green algae (Fig. 3A). This second phase in ecological change could even have been caused by further increased human impact but climatic changes cannot be ruled out either.

6.2. Environmental and hydroclimatic changes inferred from changes in lipid biomarker abundance and δD values

6.2.1. Terrestrial biomarker flux into the sediment

At 2695 varve years BP, about 60 years after the increase in varve thickness (Fig. 2) (Martin-Puertas et al., 2012b), our lipid biomarker record showed an increased influx of leaf wax *n*-alkanes into the sediment (Fig. 2B). This doubling in lipid biomarker flux occurred simultaneous with an increase in Titanium counts, a proxy for surface runoff (Fig. 2) (Martin-Puertas et al., 2012b). At the same time, tree pollen decreased significantly (from 90 to 71%) and grass and other herbaceous pollen increased from 10 to 29% (Fig. 3A). We interpret these changes in the pollen record to reflect a shift toward a more open landscape, which might have led to increased erosion and flux of terrestrial material into the lake. This is supported by the observation that the influx of terrestrial biomarkers reached its maximum at the same time when the tree/herb pollen ratios showed their lowest value at ca. 2610 varve years BP. However, the onset of the tree pollen decline (from 96 to 86%) and increasing grass pollen (from 4 to 14%) occurred already 100 years earlier, at ca. 2800 varve years BP. Also, varve thickness increased likely because of windier conditions already ca. 60 years before the increased terrestrial lipid biomarker influx at 2760 varve years BP.

The decadal resolution of our lipid biomarker and palynological data allows a detailed assessment of the temporal succession of proxy changes related to the HCO. We have to note that the different vegetation proxies presented here (alkanes, pollen) partly may reflect different source areas. While most of the *n*-alkanes likely were derived from vegetation growing on the lake shore, pollen assemblages may also include a signal from the upland vegetation surrounding the MFM crater. However, the specific catchment-conditions of lake MFM, with its steep crater walls and small catchment area, make it most likely that most pollen is derived from the catchment vegetation itself, and that the contribution of long distance transport is of minor importance (Engels et al., 2016b; Litt et al., 2009). The initial change in the pollen diagram observed at ca. 2800 varve years BP is not linked to additional transport of terrestrial material into the lake. Only at ca. 2700 varve years BP, when the largest vegetation change occurred, soil erosion increased. The first decrease in pollen concentrations at 2800 varve years BP may be due to decreased pollen production as a result of increased ecological stress, instead of changes in vegetation, which may have followed a few decades later.

6.2.2. Biomarker δD values as recorders of hydroclimate

In addition to the long-term trend to more negative δD values between 3200 and 2000 varve years BP (Fig. 2A), evident in nearly all analyzed biomarkers (except nC_{29}), aquatic and terrestrial lipid biomarker δD values showed their most substantial decrease (by between 30 and 4‰) during the HCO interval (Fig. 4).

While the 4–20‰ decrease in δD_{terr} values could have been caused by a combination of cooler conditions and lower plant transpiration (Craig, 1965; Flanagan et al., 1991; Kahmen et al., 2013b; Sachse et al., 2012) under the more humid conditions suggested by earlier studies (van Geel et al., 1996), it remains difficult to explain the rapid decline in δD_{aq} values between 22 and 30‰, as these would not be affected by changes in terrestrial transpiration.

While a decrease in air temperature would lead to more negative precipitation δD values, the observed decrease of 22–30‰ in δD_{aq} would imply an unrealistic temperature decrease between 11 and 15 °C during the HCO, when considering the modern temperature sensitivity of precipitation δD in this region (2‰/°C (IAEA/WMO, 2006);). While no temperature reconstructions are available for the HCO, a temperature decrease between 0.5 and 1.5 °C has been suggested for similar solar minima (Martin-Puertas et al., 2012b). Therefore, a potential 0.5–1.5 °C decrease during the HCO would only have had a minimal effect on precipitation δD values. However, a decrease in temperature may also be associated to shifts in the moisture source region and/or changes in moisture source temperature, which may have exercised additional control on decreasing δD values. For example, Martin-Puertas et al. (2012b) suggested a reduced atmospheric pressure gradient between the subtropics and Iceland for the HCO, resembling a negative phase of the North Atlantic Oscillation (NAO), which today results in more negative winter δD_{precip} values in parts of western Europe (Baldini et al., 2008). However, we do not observe an increase in δD values after the HCO, suggesting the observed change was not an excursion or phase but rather a shift of atmospheric conditions to a new regime.

While the relatively small changes in δD_{terr} can be largely explained by the proposed long-term hydroclimatic changes during this period, the abrupt changes in δD_{aq} of up to 30‰ over 180 years are difficult to reconcile with this scenario. Due to the absence of other proxy indicators suggesting hydroclimatic changes that could explain such a decline in δD_{aq}, we explore the possibility that factors additional to hydroclimate influenced δD_{aq}.

6.2.3. The effect of lake ecosystem changes on δD values of aquatic n-alkanes

Additional factors known to affect δD_{aq} include changes in water salinity, light intensity, growth rate and species changes (Sachs,

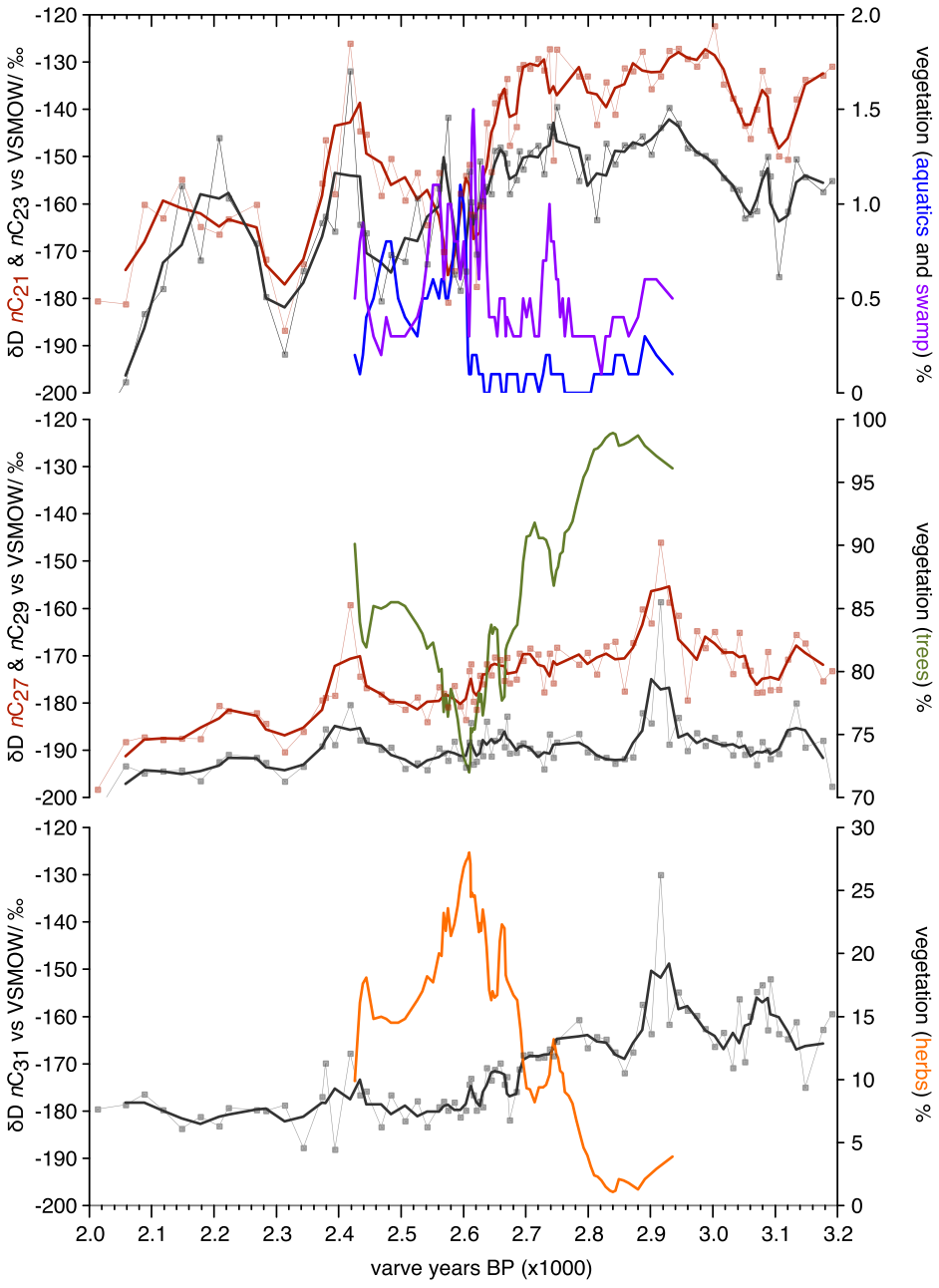

Fig. 4. Aquatic and terrestrial plant derived sedimentary *n*-alkane δD record combined with reconstructed vegetation distribution. Vegetation data shown as moving average over 3 data points. (A) Aquatic plant derived *n*-alkane δD records (nC_{21}, nC_{23}) vs. vegetation population of aquatic and swamp taxa. (B) Terrestrial plant (tree) derived *n*-alkane δD records (nC_{27}, nC_{29}) vs. tree population. (C) Terrestrial plant (herbs) derived *n*-alkane δD record (nC_{31}) vs. herb population.

2014; Zhang and Sachs, 2007). MFM always was a freshwater lake, so that we can rule out salinity as a driver. Increased upland erosion and a subsequent delivery of nutrients into the lake may have resulted in increasing growth rates of aquatic organisms. However, for aliphatic lipids produced by algae D/H fractionation does not seem to change significantly with growth rate (Sachs, 2014), and no such data exist for aquatic plants.

However, palynological data indicate significant changes in the aquatic ecosystem at 2625 varve years BP, when the total amount of aquatic and swamp taxa pollen/remains started to increase from virtually zero to a maximum of 1.5% at 2600 varve years BP (Fig. 4). Strikingly, this increase, as well as the change in species composition, was synchronous to the largest changes in nC_{21} and nC_{23} alkane δD values (Fig. 4). These compounds are primarily synthesized by aquatic organisms, likely aquatic macrophytes (Aichner et al., 2010; Cranwell et al., 1987). A minor decrease was also observed for nC_{25} δD (Fig. 2) values, a compound that can originate from both aquatic as well as terrestrial sources (Baas et al., 2000; Eglinton and Hamilton, 1967; Ficken et al., 2000). Palynological analysis indicates the occurrence/increase of *Myriophyllum spicatum/verticillatum-type* (submerged aquatic plant), *Botryococcus*, *Pediastrum* and *Tetraedron minimum* (green algae) during and after the HCO (Fig. 3). The most abundant aquatic taxon identified from the microfossil record is *Botryococcus* (identified by vegetative cell walls). As such, the available palynological data indicate major changes in the aquatic ecosystem at 2625 varve years BP, coeval

with the largest change in δD_{aq} values. Since nC_{21} and nC_{23} alkanes can be produced by a variety of different algae and submerged aquatic macrophytes (Aichner et al., 2010; Ficken et al., 2000; Gelpi et al., 1970; Parrish, 1988) it is possible that a change in the predominant aquatic organisms, characterized by different magnitudes of ε_{bio}, was at least partly responsible for the observed changes. For the more ubiquitous nC_{16} alkanoic acid differences in ε_{bio} of up to 160‰ between different green algal taxa have been observed in culture studies (Zhang and Sachs, 2007). As such, if the spectrum of organisms producing nC_{21} and nC_{23} was relatively small, which is supported by the limited number of pollen of aquatic taxa (Fig. 3), it is conceivable that changes in the predominant nC_{21} and nC_{23} producers have resulted in a significant variation within the sedimentary δD_{aq} record.

Therefore, we argue that the change in the δD values of the nC_{21} and nC_{23} alkanes does not only reflect hydroclimatic changes, but that it was amplified as a result of a change in aquatic lipid sources. This also implies that without knowledge of the biosynthetic fractionation factors for the individual nC_{21} and nC_{23} producers, a direct reconstruction of source water δD values is impossible. Arguably, the observed changes in the aquatic ecosystem were most probably initiated by the climatic and environmental changes. We suggest that the increasing influx of terrestrial material between 2695 and 2610 varve years BP due to wetter conditions and decreasing tree cover (see section 6.2.1), delivered more nutrients into the lake, acting as a fertilizer for aquatic plants. The increase in abundance of aquatic organisms around 2640 varve years BP occurred 60 years after the increase of terrestrial biomarker flux into the lake, possibly marking a threshold in the fertilization rate and triggering the diversification of the aquatic ecosystem.

6.2.4. The effect of vegetation changes on δD values of terrestrial n-alkanes

δD values of the terrestrial plant derived nC_{27}, nC_{29} and nC_{31} *n*-alkanes decreased in total by 15, 4 and 20‰, respectively, during the HCO interval (difference between mean δD values from before and after the HCO) (Fig. 2).

While changes in nC_{27} and nC_{29} δD values were gradual and can be explained by hydroclimatic changes (i.e. cooler and more humid conditions), the first larger and relatively abrupt decrease within the HCO of about 7‰ observed for nC_{31} at 2685 varve years BP coincides with the onset of a 20% increase in grass and other herbaceous pollen (Fig. 3) likely caused by an increase of human impact (Kubitz, 2000). As such, the change in δD values of nC_{31} may have been amplified by changes in terrestrial vegetation and influenced not only by climatic but also by anthropogenic factors. While nC_{31} is produced by different tree species (e.g. *Betula, Acer* (Diefendorf et al., 2011)) it is often found in higher concentrations in grasses (Massimo, 1996). Therefore, the more negative δD values after 2680 varve years BP may reflect at least partly the increased amount of grass-derived nC_{31} into the lake sediment, as *n*-alkane δD values from grasses are usually found to be more negative (up to 30‰) compared to those from trees (Duan and He, 2011; Hou et al., 2007; Kahmen et al., 2013b; Liu et al., 2006; Sachse et al., 2012).

Based on the palynological data we suggest that the nC_{27} and nC_{29} alkanes in the MFM sediments were primarily produced by trees such as *Alnus*, *Betula*, *Salix*, *Fagus*, *Carpinus*, *Ulmus* and *Quercus*, species known to produce the *n*-alkanes (Diefendorf et al., 2011; Piasentier et al., 2000; Sachse et al., 2006). Interestingly, nC_{29} δD values from the MFM sediments of the analyzed period were on average 18‰ more negative than nC_{27} and nC_{31} δD values. This consistent offset possibly implies a different water source or a different ε_{bio} for all or the major nC_{29} source organisms. The pollen record provides evidence for a high proportion of *Alnus* and *Salix* in the catchment area, taxa primarily adapted to wetter areas such as lake shores and riversides (Landolt and Bäumler, 2010; Lauber and Wagner, 2001). *Alnus* and *Salix* have been found to synthesize higher amounts of nC_{29} (Diefendorf et al., 2011; Sachse et al., 2006) and therefore the more negative nC_{29} δD values may be due to the preferred location at the lakeshore within the crater, where higher relative humidity (due to the proximity of the water body) may have resulted in smaller leaf water isotope enrichment (Craig, 1965; Farquhar et al., 2007; Flanagan et al., 1991; Kahmen et al., 2011, 2013b).

Due to the wide variety of possible sources of the nC_{27} and nC_{29} alkanes, it is likely that these compounds had the highest integrative capacity and the occurrence or disappearance of single species did not significantly affect the sedimentary δD record. As such δD values of these compounds more faithfully recorded the long-term late Holocene hydroclimatic trend to cooler and wetter conditions. Nevertheless, while less susceptible to changes than species-poor assemblages, major environmental perturbances such as human impact on vegetation, wildfires, etc, can significantly affect diverse and species-rich plant assemblages to the extent that *n*-alkane records (and their stable isotope records) can be affected.

7. Conclusions

Our combined high-resolution hydroclimate and vegetation study based on lipid biomarker δD and palynological records from lake MFM provides detailed insights into the succession of climate and ecosystem change and emphasizes the advantages of a multi-proxy approach for hydroclimate reconstructions during periods of ecological change. Specifically, our results indicate that:

(1) Between 3200 and 2000 varve years BP decreasing lipid biomarker δD values reflect the overall late Holocene trend to cooler and/or wetter conditions.
(2) Since lipid biomarker δD values remain more negative after the HCO, we suggest that this period does not only constitute a temporal climatic oscillation triggered by a grand solar minimum, but marks a transition phase resulting in the permanent establishment of cooler and wetter conditions and/or different atmospheric moisture pathways.
(3) Our data show that the local aquatic ecosystem composition did change significantly at 2640 varve years BP, ca. 60 years after the onset of changes in the terrestrial ecosystem. This is possibly induced by increased nutrient input due to enhanced soil erosion, which in turn was related to a decrease in vegetation caused by forest clearance.
(4) We argue that changes in the source organisms of aquatic *n*-alkanes (possibly associated with different degrees of biosynthetic hydrogen isotope fractionation) at the time of major (aquatic) ecosystem change caused significant changes in δD_{aq} values. Therefore, the appearance and/or disappearance of a single species can result in significant variations in sedimentary δD_{aq}, in particular for lake systems with a limited number of aquatic *n*-alkane source organisms. However, while *n*-alkane spectra of species-poor assemblages might be more susceptible to taxonomic turnover, even changes in species-rich assemblages could significantly affect the *n*-alkane record. As such, changes in the aquatic lipid biomarker δD values during the study period do not only reflect hydroclimate changes but also reflect ecological change, in our case amplifying the climatic signal.
(5) In contrast, terrestrial higher plant derived leaf wax *n*-alkanes, produced by a number of different broadleaved tree species and derived from thousands of individual trees in the lake catchment, record an integrated signal of the terrestrial

vegetation and, therefore a more reliable hydroclimate record.

Our data suggest the importance to consider the different integrative capacities of source specific vs. less specific lipid biomarkers and show that the combination with microfossil records can provide detailed insights into the succession of climatic and ecosystem changes in the lake catchment.

Acknowledgements

This work was supported by a DFG Emmy-Noether grant to DS (SA1889/1-1). It is a contribution to the INTIMATE project, which was funded as an EU COST Action and to the Helmholtz Association (HGF) Climate Initiative "REKLIM" Topic 8 'Rapid climate change derived from proxy data' and has used infrastructure of the HGF TERENO programme. Laboratory assistance was provided by Nikolas Werner (UP).

Author contributions

O. Rach carried out the *n*-alkane extraction, analysis, stable isotope measurement, isotope data evaluation and wrote the paper. S. Engels and B. van Geel carried out the pollen analysis, pollen data evaluation and wrote the paper. A. Kahmen provided infrastructure for isotope measurement, contributed to the analysis, data evaluation and writing. A. Brauer was responsible for lake coring, data evaluation and writing. C. Martín-Puertas provided the chronology and stratigraphy, contributed to data evaluation and wrote the paper. Dirk Sachse conceived the research, acquired financial support and wrote the paper.

Appendix A. Supplementary data

Supplementary data related to this article can be found at http://dx.doi.org/10.1016/j.quascirev.2017.07.019.

References

Aichner, B., Herzschuh, U., Wilkes, H., Vieth, A., Böhner, J., 2010. δD values of n-alkanes in Tibetan lake sediments and aquatic macrophytes - a surface sediment study and application to a 16 ka record from Lake Koucha. Org. Geochem. 41, 779–790.

Atwood, A.R., Sachs, J.P., 2014. Separating ITCZ- and ENSO-related rainfall changes in the Galápagos over the last 3 kyr using D/H ratios of multiple lipid biomarkers. Earth Planet. Sci. Lett. 404, 408–419.

Baas, M., Pancost, R., van Geel, B., Sinninghe Damsté, J.S., 2000. A comparative study of lipids in *Sphagnum* species. Org. Geochem. 31, 535–541.

Baldini, L.M., McDermott, F., Foley, A.M., Baldini, J.U.L., 2008. Spatial variability in the European winter precipitation δ18O-NAO relationship: implications for reconstructing NAO-mode climate variability in the Holocene. Geophys. Res. Lett. 35, L04709.

Behre, K.-E., 1981. The interpretation of anthropogenic indicators in pollen diagrams. Pollen Spores 23, 225–245.

Beug, H.J., 2004. Leitfaden der Pollenbestimmung für Mitteleuropa und angrenzende Gebiete. Verlag Dr. Friedrich Pfeil.

Brauer, A., Endres, C., Günter, C., Litt, T., Stebich, M., Negendank, J.F.W., 1999a. High resolution sediment and vegetation responses to Younger Dryas climate change in varved lake sediments from Meerfelder Maar, Germany. Quat. Sci. Rev. 18, 321–329.

Brauer, A., Endres, C., Negendank, J.F.W., 1999b. Lateglacial calendar year chronology based on annually laminated sediments from Lake Meerfelder Maar, Germany. Quat. Int. 61, 17–25.

Brauer, A., Endres, C., Zolitschka, B., Negendank, J.F.W., 2000. AMS Radiocarbin and varve chronology from the annually laminated sediment record of lake Meerfelder Maar, Germany. Radiocarbon 42, 355–368.

Brauer, A., Haug, G.H., Dulski, P., Sigman, D.M., Negendank, J.F.W., 2008. An abrupt wind shift in western Europe at the onset of the Younger Dryas cold period. Nat. Geosci. 1, 520–523.

Craig, G.L., 1965. Deuterium and oxygen 18 variations in the ocean and the marine atmosphere. In: Tongiori, E. (Ed.), Stable Isotopes in Oceanographic Studies and Paleotemperatures. CNR Lab. Geol. Nucl., Pisa, pp. 9–130.

Cranwell, P.A., Eglinton, G., Robinson, N., 1987. Lipids of aquatic organisms as potential contributors to lacustrine sediments-II. Org. Geochem. 11, 513–527.

Dansgaard, W., 1964. Stable isotopes in precipitation. Tellus 16, 436–468.

Diefendorf, A.F., Freeman, K.H., Wing, S.L., Graham, H.V., 2011. Production of n-alkyl lipids in living plants and implications for the geologic past. Geochimica Cosmochimica Acta 75, 7472–7485.

Duan, Y., He, J.X., 2011. Distribution and isotopic composition of n-alkanes from grass, reed and tree leaves along a latitudinal gradient in China. Geochem. J. 45, 199–207.

Eglinton, G., Hamilton, R.J., 1967. Leaf epicuticular waxes. Science 156, 1322–1327.

Eglinton, T.I., Eglinton, G., 2008. Molecular proxies for paleoclimatology. Earth Planet. Sci. Lett. 275, 1–16.

Engels, S., Bakker, M., Bohncke, S., Cerli, C., Hoek, W., Jansen, B., Peters, T., Renssen, H., Sachse, D., Aken, J.v., Bos, V.v.d., Geel, B.v., Oostrom, R.v., Winkels, T., Wolma, M., 2016a. Centennial-scale lake-level lowstand at Lake Uddelermeer (The Netherlands) indicates changes in moisture source region prior to the 2.8-kyr event. Holocene 26, 1075–1091.

Engels, S., Brauer, A., Buddelmeijer, N., Martín-Puertas, C., Rach, O., Sachse, D., van Geel, B., 2016b. Subdecadal-scale vegetation responses to a previously unknown late-Allerød climate fluctuation and Younger Dryas cooling at Lake Meerfelder Maar (Germany). J. Quat. Sci. 31, 741–752.

Faegri, K., Iversen, J., Kaland, P.E., Krzywinski, K., 1990. Textbook of Pollen Analysis, fourth ed. John Wiley & Sons, Ltd, Chichester.

Farquhar, G.D., Cernusak, L.A., Barnes, B., 2007. Heavy water fractionation during transpiration. Plant Physiol. 143, 11–18.

Feakins, S.J., Kirby, M.E., Cheetham, M.I., Ibarra, Y., Zimmerman, S.R.H., 2014. Fluctuation in leaf wax D/H ratio from a southern California lake records significant variability in isotopes in precipitation during the late Holocene. Org. Geochem. 66, 48–59.

Ficken, K.J., Li, B., Swain, D.L., Eglinton, G., 2000. An n-alkane proxy for the sedimentary input of submerged/floating freshwater aquatic macrophytes. Org. Geochem. 31, 745–749.

Flanagan, L.B., Comstock, J.P., Ehleringer, J.R., 1991. Comparison of modeled and observed environmental influences on the stable oxygen and hydrogen isotope composition of leaf water in *Phaseolus vulgaris*. Plant Physiol. 96, 588–596.

Gao, L., Edwards, E.J., Zeng, Y.B., Huang, Y.S., 2014. Major evolutionary trends in hydrogen isotope fractionation of vascular plant leaf waxes. PLos One 9.

Gao, L., Hou, J., Toney, J., MacDonald, D., Huang, Y., 2011. Mathematical modeling of the aquatic macrophyte inputs of mid-chain n-alkyl lipids to lake sediments: implications for interpreting compound specific hydrogen isotopic records. Geochimica Cosmochimica Acta 75, 3781–3791.

Garcin, Y., Schwab, V.F., Gleixner, G., Kahmen, A., Todou, G., Sene, O., Onana, J.M., Achoundong, G., Sachse, D., 2012. Hydrogen isotope ratios of lacustrine sedimentary n-alkanes as proxies of tropical African hydrology: insights from a calibration transect across Cameroon. Geochimica Cosmochimica Acta 79, 106–126.

Gat, J.R., 1996. Oxygen and Hydrogen isotopes in the hydrologic cycle. Annu. Rev. Earth Planet. Sci. 24, 225–262.

Gat, J.R., Mook, W.G., Meijer, H.A.J., 2000. Environmental Isotopes in the Hydrological Cycle - Principles and Applications - Volume 2: Atmospheric Water, Atmospheric Water. International Atomic Energy Agency and United Nations Educational, Scientific and Cultural Organization, Paris Vienna.

Gelpi, E., Schneider, H., Mann, J., Oro, J., 1970. Hydrocarbons of geochemical significance in microscopic algae. Phytochemistry 9, 603–612.

Hou, J., D'Andrea, W.J., MacDonald, D., Huang, Y., 2007. Hydrogen isotopic variability in leaf waxes among terrestrial and aquatic plants around Blood Pond, Massachusetts (USA). Org. Geochem. 38, 977–984.

Huang, Y., Shuman, B., Wang, Y., Webb, T., 2004. Hydrogen isotope ratios of individual lipids in lake sediments as novel tracers of climatic and environmental change: a surface sediment test. J. Paleolimnol. 31, 363–375.

IAEA/WMO, 2006. Global Network of Isotopes in Precipitation. The GNIP Database, Bundesanstalt fuer Gewaesserkunde.

Kahmen, A., Hoffmann, B., Schefuss, E., Arndt, S.K., Cernusak, L.A., West, J.B., Sachse, D., 2013a. Leaf water deuterium enrichment shapes leaf wax n-alkane delta D values of angiosperm plants II: observational evidence and global implications. Geochimica Cosmochimica Acta 111, 50–63.

Kahmen, A., Sachse, D., Arndt, S.K., Tu, K.P., Farrington, H., Vitousek, P.M., Dawson, T.E., 2011. Cellulose delta(18)O is an index of leaf-to-air vapor pressure difference (VPD) in tropical plants. Proc. Natl. Acad. Sci. 108, 1981–1986.

Kahmen, A., Schefuss, E., Sachse, D., 2013b. Leaf water deuterium enrichment shapes leaf wax n-alkane delta D values of angiosperm plants I: experimental evidence and mechanistic insights. Geochimica Cosmochimica Acta 111, 39–49.

Killops, S., Killops, V., 2005. Introduction to Organic Geochemistry, second ed. Blackwell Publishing, Malden (USA), Oxford (UK), Carlton (Australia).

Kubitz, B., 2000. History of Holocene Vegetation and Human Settlement in Western Eifel (Germany) Based on a High-resolution Pollen Diagram from the Meerfelder Maar Lake, pp. 1–106 [Dissertationes Botanicae. History of Holocene vegetation and human settlement in Western Eifel. J. Cramer in der Gebrueder Borntraeger Verlagsbuchhandlung, D-14129, Berlin, Germany.

Landolt, E., Bäumler, B., 2010. Flora indicativa: ökologische Zeigerwerte und biologische Kennzeichen zur Flora der Schweiz und der Alpen. In: des Conservatoire et Jardin botaniques de la ville de Genève.

Lauber, K., Wagner, G., 2001. In: Auflage (Ed.), Flora Helvetica, vol. 3. Verlag Paul Haupt, Bern; Stuttgart; Wien.

Litt, T., Brauer, A., Goslar, T., Merkt, J., Balaga, K., Müller, H., Ralska-Jasiewiczowa, M., Stebich, M., Negendank, J.F.W., 2001. Correlation and synchronisation of

Lateglacial continental sequences in northern central Europe based on annually laminated lacustrine sediments. Quat. Sci. Rev. 20, 1233–1249.
Litt, T., Scholzel, C., Kuhl, N., Brauer, A., 2009. Vegetation and climate history in the Westeifel Volcanic Field (Germany) during the past 11000 years based on annually laminated lacustrine maar sediments. Boreas 38, 679–690.
Liu, W.G., Yang, H., Li, L.W., 2006. Hydrogen isotopic compositions of n-alkanes from terrestrial plants correlate with their ecological life forms. Oecologia 150, 330–338.
Magny, M., 1993. Solar influences on Holocene climate changes illustrated by correlations between past lake-level fluctuations and the atmospheric C14 record. Quat. Res. 40, 1–9.
Marcott, S.A., Shakun, J.D., Clark, P.U., Mix, A.C., 2013. A reconstruction of regional and global temperature for the past 11,300 years. Science 339, 1198–1201.
Martin-Puertas, C., Brauer, A., Dulski, P., Brademann, B., 2012a. Testing climate-proxy stationarity throughout the Holocene: an example from the varved sediments of Lake Meerfelder Maar (Germany). Quat. Sci. Rev. 58, 56–65.
Martin-Puertas, C., Matthes, K., Brauer, A., Muscheler, R., Hansen, F., Petrick, C., Aldahan, A., Possnert, G., van Geel, B., 2012b. Regional atmospheric circulation shifts induced by a grand solar minimum. Nat. Geosci. 5, 397–401.
Massimo, M., 1996. Chemotaxonomic significance of leaf wax alkanes in the Gramineae. Biochem. Syst. Ecol. 24, 53–64.
McInerney, F.A., Helliker, B.R., Freeman, K.H., 2011. Hydrogen isotope ratios of leaf wax n-alkanes in grasses are insensitive to transpiration. Geochimica Cosmochimica Acta 75, 541–554.
Moore, P.D., Webb, J.A., Collinson, M.E., 1991. Pollen Analysis, second ed. Blackwell Scientific Publications, 3 Cambridge Center, Cambridge, Massachusetts 02142, USA Osney Mead, Oxford OX2 0EL, England.
Moschen, R., Lucke, A., Schleser, G.H., 2005. Sensitivity of biogenic silica oxygen isotopes to changes in surface water temperature and palaeoclimatology. Geophys. Res. Lett. 32.
Movius, H.L., 2013. The Irish Stone Age. Cambridge University Press.
Nelson, D.M., Henderson, A.K., Huang, Y.S., Hu, F.S., 2013. Influence of terrestrial vegetation on leaf wax delta D of Holocene lake sediments. Org. Geochem. 56, 106–110.
Parrish, C.C., 1988. Dissolved and particulate marine lipid classes - a review. Mar. Chem. 23, 17–40.
Peters, K.E., Moldowan, J.M., Walters, C.C., 2007. The Biomarker Guide: Volume 1, Biomarkers and Isotopes in the Environment and Human History. Cambridge University Press.
Piasentier, E., Bovolenta, S., Malossini, F., 2000. The n-alkane concentrations in buds and leaves of browsed broadleaf trees. J. Agric. Sci. 135, 311–320.
Rach, O., Brauer, A., Wilkes, H., Sachse, D., 2014. Delayed hydrological response to Greenland cooling at the onset of the Younger Dryas in western Europe. Nat. Geosci. 7, 109–112.
Reimer, P.J., Baillie, M.G.L., Bard, E., Bayliss, A., Beck, J.W., Blackwell, P.G., Ramsey, C.B., Buck, C.E., Burr, G.S., Edwards, R.L., Friedrich, M., Grootes, P.M., Guilderson, T.P., Hajdas, I., Heaton, T.J., Hogg, A.G., Hughen, K.A., Kaiser, K.F., Kromer, B., McCormac, F.G., Manning, S.W., Reimer, R.W., Richards, D.A., Southon, J.R., Talamo, S., Turney, C.S.M., van der Plicht, J., Weyhenmeye, C.E., 2009. Intcal09 and Marine09 radiocarbon age clibration curves, 0-50.000 years cal BP. Radiocarbon 51, 1111–1150.
Renssen, H., Seppä, H., Heiri, O., Roche, D.M., Goosse, H., Fichefet, T., 2009. The spatial and temporal complexity of the Holocene thermal maximum. Nat. Geosci. 2, 410–413.
Sachs, J.P., 2014. Hydrogen isotope signatures in the lipids of phytoplankton. In: Holland, H.D., Turekian, K.K. (Eds.), Treatise on Geochemistry, second ed. Elsevier, Oxford, pp. 79–94.
Sachs, J.P., Pahnke, K., Smittenberg, R., Zhang, Z., 2013. Biomarker indicators of past climate. In: Mock, S.A.E.J. (Ed.), Encyclopedia of Quaternary Science, second ed. Elsevier, Amsterdam, pp. 775–782.
Sachs, J.P., Sachse, D., Smittenberg, R.H., Zhang, Z.H., Battisti, D.S., Golubic, S., 2009. Southward movement of the Pacific intertropical convergence zone AD 1400-1850. Nat. Geosci. 2, 519–525.
Sachse, D., Billault, I., Bowen, G.J., Chikaraishi, Y., Dawson, T.E., Feakins, S.J., Freeman, K.H., Magill, C.R., McInerney, F.A., van der Meer, M.T.J., Polissar, P., Robins, R.J., Sachs, J.P., Schmidt, H.-L., Sessions, A.L., White, J.W.C., West, J.B., Kahmen, A., 2012. Molecular paleohydrology: interpreting the hydrogen-isotopic composition of lipid biomarkers from photosynthesizing organisms. Annu. Rev. Earth Planet. Sci. 40, 221–249.
Sachse, D., Radke, J., Gleixner, G., 2004. Hydrogen isotope ratios of recent lacustrine sedimentary n-alkanes record modern climate variability. Geochimica Cosmochimica Acta 68, 4877–4889.
Sachse, D., Radke, J., Gleixner, G., 2006. δD values of individual n-alkanes from terrestrial plants along a climatic gradient - implications for the sedimentary biomarker record. Org. Geochem. 37, 469–483.
Sachse, D., Sachs, J.P., 2008. Inverse relationship between D/H fractionation in cyanobacterial lipids and salinity in Christmas Island saline ponds. Geochimica Cosmochimica Acta 72, 793–806.
Sauer, P.E., Eglinton, T.I., Hayes, J.M., Schimmelmann, A., Sessions, A.L., 2001. Compound-specific D/H ratios of lipid biomarkers from sediments as a proxy for environmental and climatic conditions. Geochimica Cosmochimica Acta 65, 213–222.
Schefuss, E., Kuhlmann, H., Mollenhauer, G., Prange, M., Pätzold, J., 2011. Forcing of wet phases in southeast Africa over the past 17,000 years. Nature 480, 509–512.
Scott, E.M., Alekseev, A.Y., Zaitseva, G., 2006. Impact of the environment on human migration in eurasia. In: Proceedings of the NATO Advanced Research Workshop, Held in St. Petersburg, 15–18 November 2003. Springer Netherlands.
Sessions, A.L., Burgoyne, T.W., Schimmelmann, A., Hayes, J.M., 1999. Fractionation of hydrogen isotopes in lipid biosynthesis. Org. Geochem. 30, 1193–1200.
Sessions, A.L., Hayes, J.M., 2005. Calculation of hydrogen isotopic fractionations in biogeochemical systems. Geochimica Cosmochimica Acta 69, 593–597.
Smittenberg, R.H., Saenger, C., Dawson, M.N., Sachs, J.P., 2011. Compound-specific D/H ratios of the marine lakes of Palau as proxies for West Pacific Warm Pool hydrologic variability. Quat. Sci. Rev. 30, 921–933.
Stockmarr, J., 1971. Tablets with spores used in absolute pollen analysis. Pollen Spores 13, 615–621.
Swierczynski, T., Lauterbach, S., Dulski, P., Delgado, J., Merz, B., Brauer, A., 2013. Mid- to late Holocene flood frequency changes in the northeastern Alps as recorded in varved sediments of Lake Mondsee (Upper Austria). Quat. Sci. Rev. 80, 78–90.
Tierney, J.E., Oppo, D.W., Rosenthal, Y., Russell, J.M., Linsley, B.K., 2010. Coordinated hydrological regimes in the Indo-Pacific region during the past two millennia. Paleoceanography 25.
Tierney, J.E., Russell, J.M., Huang, Y.S., Sinninghe Damsté, J.S., Hopmans, E.C., Cohen, A.S., 2008. Northern hemisphere controls on tropical southeast African climate during the past 60,000 years. Science 322, 252–255.
Van Geel, B., 1978. A palaeoecological study of holocene peat bog sections in Germany and The Netherlands, based on the analysis of pollen, spores and macro- and microscopic remains of fungi, algae, cormophytes and animals. Rev. Palaeobot. Palynology 25, 1–120.
van Geel, B., Berglund, B.E., 2000. A causal link between a climatic deterioration around 850 cal BC and a subsequent rise in human population density in NW-Europe? Terra Nostra 7, 126–130.
van Geel, B., Buurman, J., Waterbolk, H.T., 1996. Archaeological and palaeoecological indications of an abrupt climate change in The Netherlands, and evidence for climatological teleconnections around 2650 BP. J. Quat. Sci. 11, 451–460.
van Geel, B., Engels, S., Martin-Puertas, C., Brauer, A., 2013. Ascospores of the parasitic fungus *Kretzschmaria deusta* as rainstorm indicators during a late Holocene beech-forest phase around lake Meerfelder Maar, Germany. J. Paleolimnol. 50, 33–40.
van Geel, B., Raspopov, O.M., Renssen, H., van der Plicht, J., Dergachev, V.A., Meijer, H.A.J., 1999. The role of solar forcing upon climate change. Quat. Sci. Rev. 18, 331–338.
Vonmoos, M., Beer, J., Muscheler, R., 2006. Large variations in holocene solar activity: constraints from Be-10 in the Greenland ice core project ice core. J. Geophys. Research-Space Phys. 111.
Wanner, H., Beer, J., Butikofer, J., Crowley, T.J., Cubasch, U., Fluckiger, J., Goosse, H., Grosjean, M., Joos, F., Kaplan, J.O., Kuttel, M., Muller, S.A., Prentice, I.C., Solomina, O., Stocker, T.F., Tarasov, P., Wagner, M., Widmann, M., 2008. Mid- to Late Holocene climate change: an overview. Quat. Sci. Rev. 27, 1791–1828.
Wirth, S.B., Glur, L., Gilli, A., Anselmetti, F.S., 2013. Holocene flood frequency across the Central Alps – solar forcing and evidence for variations in North Atlantic atmospheric circulation. Quat. Sci. Rev. 80, 112–128.
Zhang, Z., Leduc, G., Sachs, J.P., 2014. El Niño evolution during the Holocene revealed by a biomarker rain gauge in the Galápagos Islands. Earth Planet. Sci. Lett. 404, 420–434.
Zhang, Z., Sachs, J.P., 2007. Hydrogen isotope fractionation in freshwater algae: I. Variations among lipids and species. Org. Geochem. 38, 582–608.
Zolitschka, B., Brauer, A., Negendank, J.F.W., Stockhausen, H., Lang, A., 2000. Annually dated late Weichselian continental paleoclimate record from the Eifel, Germany. Geology 28, 783–786.
Zöller, L., Blanchard, H., 2009. The partial heat – longest plateau technique: testing TL dating of Middle and Upper Quaternary volcanic eruptions in the Eifel Area, Germany. E&G - Quat. Sci. J. 58, 86–107.